Carbohydrate Polymers 262 (2021) 117944

Contents lists available at ScienceDirect

Carbohydrate Polymers

journal homepage: www.elsevier.com/locate/carbpol

Advanced characterization of regioselectively substituted methylcellulose model compounds by DNP enhanced solid-state NMR spectroscopy

Pierrick Berruyer [a], Martin Gericke [b], Pinelopi Moutzouri [a], Dörthe Jakobi [b], Michel Bardet [a,c], Leif Karlson [d], Staffan Schantz [e], Thomas Heinze [b,*], Lyndon Emsley [a,*]

[a] Institut des Sciences et Ingénierie Chimiques, Ecole Polytechnique Fédérale de Lausanne (EPFL), CH-1015 Lausanne, Switzerland
[b] Institute of Organic Chemistry and Macromolecular Chemistry, Friedrich Schiller University of Jena, Centre of Excellence for Polysaccharide Research, Humboldtstraße 10, D-07743 Jena, Germany
[c] Univ. Grenoble Alpes, CEA, IRIG-MEM, Laboratoire de Résonance Magnétique, Grenoble 38000, France
[d] Nouryon Functional Chemicals AB, SE-444 31 Stenungsund, Sweden
[e] Oral Product Development, Pharmaceutical Technology & Development, Operations, AstraZeneca, Gothenburg, Sweden

ARTICLE INFO

Keywords:
Cellulose ethers
Regioselectivity
Methylcellulose
Structure characterization
Solid state NMR
DNP enhancement

ABSTRACT

Dynamic Nuclear Polarization MAS NMR is introduced to characterize model methylcellulose ether compounds at natural isotopic abundance. In particular an approach is provided to determine the position of the methyl ether group within the repeating unit. Specifically, natural abundance ^{13}C-^{13}C correlation experiments are used to characterize model 3-*O*-methylcellulose and 2,3-*O*-dimethylcellulose, and identify changes in chemical shifts with respect to native cellulose. We also probe the use of through space connectivity to the closest carbons to the CH_3 to identify the substitution site on the cellulose ether. To this end, a series of methylcellulose ethers was prepared by a multistep synthesis approach. Key intermediates in these reactions were 2,6-*O*-diprotected thexyldimethylsilyl (TDMS) cellulose and 6-*O*-monoprotected TDMS cellulose methylated under homogeneous conditions. The products had degrees of substitution of 0.99 (3-*O*-methylcellulose) and 2.03 (2,3-*O*-dimethylcellulose) with exclusively regioselective substitution. The approaches developed here will allow characterization of the substitution patterns in cellulose ethers.

1. Introduction

Cellulose ethers are widely exploited as additives in a broad range of applications, such as pharmaceutical formulations (Arca et al., 2018; Li, Martini, Ford, & Roberts, 2005), paint and cement based building formulations (Karlson, Joabsson, & Thuresson, 2000; Patural et al., 2011), food (Young, 2014), and drilling and mining processes (Wever, Picchioni, & Broekhuis, 2011). The overall molecular structure of cellulose ethers determines the physical properties of their products, which in return affect their efficacy. Some of the most important characteristics of commercial cellulose ethers in this perspective include the average molecular weight and the overall degree of substitution (DS) of the ether substituents. Moreover, the distribution of substituents within the repeating unit and the heterogeneity between the surface and bulk of the material are key parameters. These characteristics can, to some extent, be tuned by reaction conditions (molecular weight of the starting cellulose, amount of reagents, composition of the reaction medium, time, temperature, etc.).

The cellulose repeating unit features three different hydroxyl groups that can be functionalized, and therefore cellulose ethers with the same DS might possess a different substitution pattern, e.g. 2-*O*-, 3-*O*-, 6-*O*-substitution or non-regioselective substitution (Mischnick, 2018). For several cellulose alkyl ethers, it has been reported that the distribution of substituents within the repeating unit is an important characteristic that has a strong influence on properties such as the self-aggregation behavior (Heinze, Pfeifer, Sarbova, & Koschella, 2011; Sun et al., 2009). The characterization of commercial cellulose ethers is therefore crucial to understand their performance, and for example to ensure constant batch-to-batch quality for the polysaccharide derivatives themselves as well as the products in which they are employed. A range of techniques is conventionally used to characterize cellulose ethers, including liquid ^{1}H and ^{13}C NMR spectroscopy as well as HPLC and GC-MS chromatography after degradation of the samples into mono- or oligo-saccharide fragments (Kern et al., 2000). However, questions such

* Corresponding authors.
E-mail addresses: thomas.heinze@uni-jena.de (T. Heinze), lyndon.emsley@epfl.ch (L. Emsley).

https://doi.org/10.1016/j.carbpol.2021.117944
Received 11 January 2021; Received in revised form 12 March 2021; Accepted 12 March 2021
Available online 15 March 2021

as the distribution of ether groups *(i)* within the repeating unit, *(ii)* along the polymer chain, and *(iii)* within the bulk material as a whole, still remain elusive and novel analytical tools are in high demand.

Solid-state magic angle spinning (MAS) NMR spectroscopy could play a key role to address questions related to the molecular structure characterization, as it can probe both local molecular environments, and long-range order in materials, and has been widely used in polymers (Reif, Ashbrook, Emsley, & Hong, 2021; Schmidt-Rohr & Spiess, 1999). In the context of cellulose research, solid-state MAS NMR has been particularly successful to distinguish the different crystalline and amorphous domains in celluloses of different origins (Atalla & Vanderhart, 1984; Kono, Erata, & Takai, 2002; Kono, Numata, Erata, & Takai, 2004; Sparrman et al., 2019), but also to locate and estimate domain sizes of different phases with ^{1}H or ^{13}C spin diffusion, notably in cellulose microfibrils or plant cells (Foston, 2014; Foston, Katahira, Gjersing, Davis, & Ragauskas, 2012). During the last decade, Dynamic Nuclear Polarization (DNP) has significantly increased the sensitivity of solid-state MAS NMR (Berruyer, Emsley, & Lesage, 2018), and DNP enhanced MAS NMR has emerged as a powerful tool to study materials, including polymers (Mollica et al., 2014), and biomolecular assemblies (Elkins, Sergeyev, & Hong, 2018; Gupta et al., 2019). In the context of cellulose research, the high sensitivity provided by DNP MAS NMR enabled the characterization of microcrystalline cellulose (Takahashi et al., 2012), cellulose esters (Groszewicz et al., 2020), plant cell walls (Wang et al., 2013; Wang, Yang, Kubicki, & Hong, 2016; Zhao et al., 2021), biomass (Perras et al., 2017), lignin-polysaccharide interactions (Kang et al., 2019), and the topology of wood fibers (Viger-Gravel et al., 2019).

In this work, DNP MAS NMR is introduced to characterize model methylcellulose ether compounds at natural isotopic abundance, and in particular an approach is provided to determine the position of the methyl ether group within the repeating unit. Specifically, natural abundance ^{13}C-^{13}C correlation experiments are used to characterize the backbone of 3-*O*-methylcellulose and 2,3-*O*-dimethylcellulose, and identify changes in chemical shifts with respect to native cellulose. We also probe the use of through space connectivity to the closest carbons to the CH_3 to identify the substitution site on the cellulose ether. The approach will be useful to characterize cellulose ethers with an unknown substitution pattern.

2. Experimental

2.1. Materials

N,*N*-Dimethylacetamide (DMA), dimethylsulfoxide (DMSO), and pyridine of anhydrous grade were purchased from Acros Organics and stored as received by the supplier. All other chemicals were obtained from Sigma Aldrich and used as received. Microcrystalline cellulose (Avicel PH-101) and LiCl was purchased from Sigma Aldrich and dried prior to use under vacuum at 100 °C and 130 °C respectively. Deuterated solvents were purchased from Cambridge Isotope Laboratories. The DNP polarizing agent AMUPOL was obtained from Dr. Olivier Ouari (Aix-Marseille Université).

2.2. Measurements

Solution NMR spectra of polysaccharide derivatives were recorded at 25 °C in methanol-d_4, chloroform-d_1, DMSO-d_6 (with or without LiCl), or mixtures therefrom at concentrations of ≥ 15 mg/mL (^{1}H NMR) or ≥ for 60 mg/mL (^{13}C NMR, HSQC-DEPT) with a Bruker Avance 250 MHz or a Bruker Avance 400 MHz spectrometer. For the peak assignment, carbon atoms were numbered consecutively starting from the cellulose backbone (1–6) to the additional substituents (≥ 7) as displayed in each figure. Carbon atoms of the TDMS substituent were labeled a to e.

A VARIO EL III CHNS analyzer (Elementaranalysensysteme GmbH) was used for elemental analyses (carbon-, hydrogen-, nitrogen-, and sulfur content). The silicon content was determined gravimetrically. The samples (about 100 mg) were treated with fuming sulfuric acid in a platinum cup. The liquid was removed by heating the open cup with a Bunsen burner under a hood. After drying in an oven (500 °C), the silicon content was calculated from the differential weights under the assumption that silicon was converted into SiO_2. The degree of substitution (DS) with thexyldimethylsilyl (TDMS) groups was determined from the silicon content (Si %) according to formula 1. The DS with methyl groups (DS_{Me}) was determined from the ^{1}H NMR spectra of peracetylated samples according to formula 2 with I_1 being the integral from 1.9 to 2.3 ppm (peaks related to the methyl group in the acetyl moiety) and I_2 being the integral from 3.8 to 4.7 ppm (peaks related to the H-1 and H-6 position within the cellulose backbone).

$$DS_{TDMS} = \frac{162.1 \times Si\%/100\ \%}{28.1 - 142.2 \times Si\%/100\ \%} \quad (1)$$

$$DS_{Me} = 3 - \frac{I_1}{I_2} \quad (2)$$

2.3. DNP NMR spectroscopy

DNP Solid-State NMR was performed on a Bruker Avance III HD 400 MHz spectrometer equipped with a 263 GHz gyrotron or a 264 GHz klystron outputting continuous μwaves for DNP. The main magnetic field of the magnet was adjusted using the sweep coil to match the maximum positive DNP enhancement of the AMUPOL DNP polarizing agent. The μwaves power was optimized to get the highest DNP enhancement on the cellulose signals via CP. The spectrometer was equipped with a 3.2 mm LTMAS DNP probe in double mode configuration HX tuned to ^{1}H and ^{13}C. Typically, 15 mg of the cellulose ether were impregnated with 15 μL of a 10 mM AMUPOL in D_2O:H_2O 9:$1_{v/v}$ solution, and then transferred to a sapphire rotor sealed with a silicon plug or a Teflon insert and closed with a zirconia drive cap. The typical temperatures of the spinning samples under μwave irradiation are 105 K. The DNP enhancement is defined as the ratio of the signal area of the spectrum recorded with μwaves to the one recorded without μwaves irradiation. The error bars are estimated from the signal to noise ratio. All experimental parameters are available from the supporting information.

2.4. Synthesis

2.4.1. Synthesis of 2,6-O-di-thexyldimethylsilyl cellulose

Cellulose (100 g) was dispersed in DMA (2.5 L) and the mixture was stirred for 3 h at 130 °C. After decreasing the temperature to 100 °C, LiCl (200 g) was added and the mixture was stirred until complete dissolution occurred. Imidazole (200 g) was dissolved in the cellulose solution and TDMS chloride (500 mL) was added in portions. After stirring for 24 h at 100 °C, the reaction mixture was cooled to 25 °C and poured into water (3 L). The precipitate formed was removed by filtration, washed two-times with water (600 mL each) and five-times with ethanol (300 mL each), and finally dried at 60 °C under vacuum.

Yield: 272 g silylated product (98 % molar yield)

DS_{TDMS} = 2.01 (based on a silicon content of 12.61 %)

Elemental analysis found: C% 59.23, H% 10.29, Si % 12.61; calculated: C% 59.22, H% 10.31, Si% 12.61

^{13}C NMR (250 MHz, chloroform-d_1): δ (ppm) = 102.0 (C-1), about 75.0 (C-2, C-4, C-5), 60.3 (C-6,), 34.1 (TDSM / c), 25.1 (TDSM / b) 20.5–18.5 (TDSM / d, e), -1.6 to -3.6 (TDSM / a)

2.4.2. Synthesis of 6-O-thexyldimethylsilyl cellulose

Cellulose (60 g) was dispersed in *N*-methylpyrollidone (NMP; 250 mL) and stirred for 1 h at 80 °C. Liquid ammonia (about 350 mL) was condensed into a separate reaction vessel that was cooled to about −77 °C using dry ice / isopropanol and NMP (250 mL) was added. The

cellulose / NMP mixture was cooled to -25 °C and combined with the ammonia saturated NMP solution. After 1 h stirring at -25 °C, TDMS chloride (165 mL) was added in portions within 1 h and the reaction mixture was stirred for 1 h at -25 °C. Afterwards, the temperature was raised gradually to 40 °C within 5 h and the reaction was continued for another 24 h at 80 °C. The reaction mixture was poured into phosphate buffer (pH-value of 7; 5 L) and the precipitate was removed, washed five-times with water (5 L each) and five-times with ethanol (1.5 L each), and finally dried at 60 °C under vacuum.

Yield: 98 g silylated product (71 % molar yield)

DS_{TDSM} = 0.97 (based on a silicon content of 9.13 %)

Elemental analysis found: C% 54.28, H% 8.95, Si % 9.13; calculated: C% 55.15, H% 9.17, Si% 9.13

^{13}C NMR (250 MHz, chloroform-d_1): δ (ppm) = 103.0 (C-1), about 75.0 (C-2, C-4, C-5), 60.3 (C-6,), 34.1 (TDSM / c), 25.1 (TDSM / b) 20.3–18.5 (TDSM / d, e), -3.7 (TDSM / a)

2.4.3. Methylation of regioselectively protected cellulose derivatives (typical example)

2,6-*O*-di-TDMS cellulose (13 g) was dissolved in tetrahydrofuran (THF; 130 mL) and sodium hydride (7.6 g; 10 mol/mol modified repeating unit) was added portion wise. The suspension was stirred for 30 min under inert conditions. Methyl iodide (18.5 mL; 10 mol/mol modified repeating unit) was added and the reaction mixture was stirred for 24 h at 25 °C and subsequently for 4 d at 25 °C. The product was isolated by precipitation of the reaction mixture in water / acetic acid mixture (30 : 1; 1500 mL), washed two-times with water (500 mL each) and three-times with ethanol (500 mL each), and dried at 60 °C under vacuum.

Yield: 12.4 g product (91 % molar yield; determined for a DS_{TDMS} of 2.01 and a DS_{Me} of 0.99)

Elemental analysis found: C% 59.15, H% 10.25; calculated: C% 60.01, H% 10.43

^{13}C NMR (250 MHz, chloroform-d_1): δ (ppm) = 101.4 (C-1), 86.2 (C-$3_{methylated}$), 76.5–74.0 (C-2, C-4, C-5), 61.5–60.8 (C-6, methyl / C-7), 34.0 (TDSM / c), 25.0 (TDSM / b) 20.5–18.5 (TDSM / d, e), -1.6 to -3.7 (TDSM / a)

2.4.4. Removal of silyl protecting groups (typical example)

The silylated cellulose ether (12 g; see 2.4.3) was dissolved in THF (180 mL) and treated with tetrabutylammonium fluoride trihydrate (TBAF x 3 H_2O; 32.9 g) for 1 d at 50 °C. The solution was poured into ethanol (1 L) and the precipitate was removed by filtration, washed two-times with ethanol (200 mL each), and dried in vacuum. The intermediate product (4.5 g) was dissolved in dimethylsulfoxide (DMSO; 20 mL) and treated again with TBAF x 3 H_2O (9.0 g) for 1 d at 50 °C. The solution was poured into ethanol (300 mL) and the precipitate was removed by filtration, washed five-times with ethanol (50 mL), and dried at 60 °C under vacuum.

Yield: 4.5 g product (45 % molar yield; determined for a DS_{Me} of 0.99)

Elemental analysis found: C% 44.28, H% 7.08; calculated: C% 47.72, H% 6.81

^{13}C NMR (250 MHz, DMSO-d_6): δ (ppm) = 103.4 (C-1), 85.4 (C-$3_{methylated}$), 77.4 (C-4), 75.6 (C-5), 74.5 (C-2), 60.8 (C-6), 59.7 (methyl / C-7)

2.4.5. Peracetylation of cellulose ethers (typical example)

The cellulose ether (200 mg; see 2.4.4) was suspended in pyridine (10 mL) and 4-*N*,*N*-dimethylaminopyridine (20 mg) followed by acetic anhydride (10 mL) were added. After stirring for 24 h at 80 °C, the reaction mixture was cooled to 25 °C and poured into ethanol (400 mL). The precipitate was removed by filtration, washed four-times with ethanol (50 mL), and dried at 60 °C under vacuum.

A modified two-step-procedure was employed for the peracetylation of cellulose ethers with a low $DS_{Me} < 1.0$. The samples (200 mg) were dissolved in DMA (20 mL) and 4-*N*,*N*-dimethylaminopyridine (20 mg) followed by acetyl chloride (3 mL) were added. After stirring for 6 h at 50 °C, the reaction mixture was cooled to 25 °C and poured into ethanol (150 mL). The precipitate was removed by filtration, washed three-times with ethanol (50 mL), and dried at 60 °C under vacuum. The intermediate product was subsequently peracetylated with acetic anhydride in pyridine as described above for cellulose ethers with a $DS_{Me} \geq 1.0$.

Yield: 210 mg product (71 % molar yield; determined for a DS_{Me} of 0.99 and a $DS_{Acetate}$ of 2.01)

Elemental analysis found: C% 50.48, H% 6.36; calculated: C% 50,78, H% 6.14

^{13}C NMR (250 MHz, chloroform-d_1): δ (ppm) = 170.4–169.4 (acetyl / C-9) 100.9 (C-1), 82.5 (C-$3_{methylated}$), 72.9–72.6 (C-2, C-5), 62.2 (C-6), 60.3 (methyl / C-7), 20.9 (acetyl / C-8)

3. Results and discussion

3.1. Synthesis of reference samples

The first goal of the present study was the synthesis of cellulose methyl ethers with a well-defined molecular structure in terms of overall degree of substitution with methyl groups (DS_{Me}) and substitution pattern. Two reference samples, 3-*O*-methylcellulose (DS_{Me} = 1) and 2,3-*O*-dimethylcellulose (DS_{Me} = 2) were targeted by a multistep synthesis approach (Fig. 1.). In the first step, cellulose was fully protected, either at positions C-2 and C-6 or only at position C-6, using bulky thexyldimethylsilyl (TDMS) moieties as protecting groups (Koschella & Klemm, 1997; Koschella, Heinze, & Klemm, 2001). The resulting TDMS cellulose ethers were methylated at the remaining free hydroxyl groups to the desired DS_{Me}. Finally, the TDMS protecting groups were cleaved quantitatively from the polysaccharide backbone by conversion with fluoride ions.

Two types of regioselectively protected cellulose derivatives were prepared within this study. Conversion of cellulose dissolved in *N*,*N*-dimethylacetamide (DMA) / LiCl with TDMS chloride yielded a 2,6-*O*-TDMS cellulose with a DS_{TDMS} of 2.01. It has been demonstrated that only positions 2 and 6 are converted to TDMS ethers under these homogeneous reaction conditions (Koschella & Klemm, 1997; Koschella et al., 2001). Thus, the cellulose silyl ether obtained by completely homogeneous silylation is an ideal starting compound for the synthesis of cellulose ethers with a selective 3-*O*-substitution pattern and a maximum DS_{Me} of 1.0. For the synthesis of regioselective 2,3-*O*-dimethylcellulose, a starting cellulose derivative with a protecting group at position 6 was desired. Tritylation, i.e., etherification of cellulose with triphenylmethyl chloride or methoxy aryl analogues, has been described as an approach towards 6-*O*-protected cellulose derivatives and 2,3-*O*-substituted compounds prepared therefrom (Fox, Li, Xu, & Edgar, 2011; Kern et al., 2000; Kondo & Gray, 1991). In the present work, TDMS protecting groups were preferred due to their higher regioselectivity and in order to simplify the final deprotection steps. A 6-*O*-TDMS cellulose with a DS_{TDMS} of 0.97 was obtained in a heterogeneous process using *N*-methylpyrollidone (NMP) and liquid ammonia as the reaction medium. Under these conditions, position 6 is converted selectively with TDMS protecting groups (Koschella & Klemm, 1997; Koschella, Fenn, Illy, & Heinze, 2006).

Both TDMS celluloses were employed as starting materials for the homogeneous methylation using tetrahydrofuran (THF) as solvent, sodium hydride as base, and different amounts of methyl iodide as reagent. In both cases the possibility of having a distribution of different substitution patterns is avoided by design. The influence of the reaction conditions during the methylation step was investigated comprehensively and a detailed report is given in Table S1. It was found that the conversion of all the residual hydroxyl groups in 2,6-*O*-TDMS cellulose and 6-*O*-TDMS cellulose was achieved within 5 days of reaction (1 d at 25 °C and 4 d at 50 °C). Thus, the desired 3-*O*-methylcellulose (DS_{Me} = 2.03) and 2,3-*O*-dimethylcellulose (DS_{Me} = 0.99) could be obtained after

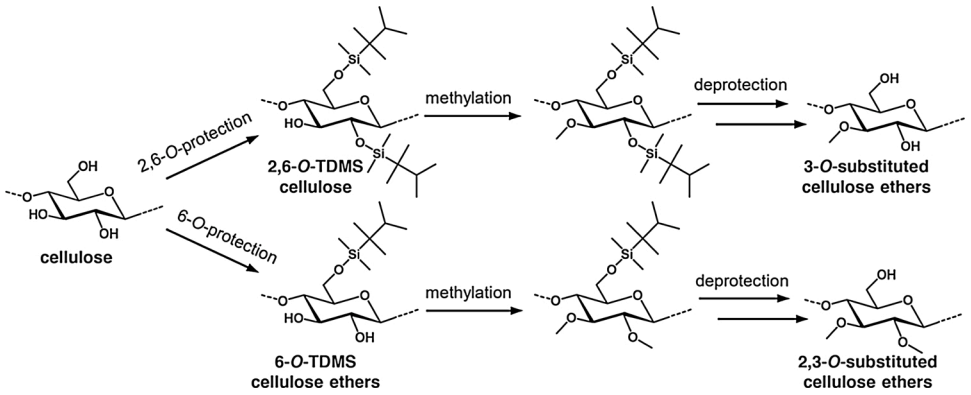

Fig. 1. Reaction scheme for the regioselective synthesis of 3-*O*-substituted and 2,3-*O*-substituted methylcelluloses.

deprotection. Moreover, methylcellulose model compounds with regioselective substitution and defined DS < 1 (3-*O*-substitued) and DS < 2 (2,3-*O*-substitued) were accessible as well by adjusting the molar ratio. The products obtained in the methylation step were purified, dissolved in THF and treated with an excess of tetrabutylammonium fluoride (TBAF) since the affinity of silicon to fluoride leads to the cleavage of the TDMS protecting groups from the polysaccharide backbone and to the release of the hydroxyl groups. Here it should be noted that the deprotection reaction always starts homogeneously and after some time precipitation of an intermediate product occurs. This is due to the fact that initially the methyl silyl mixed cellulose ethers are hydrophobic and therefore soluble in rather non-polar solvents such as THF and chloroform. However, upon partial cleavage of the hydrophobic TDMS moieties the products become increasingly hydrophilic rendering the polymers insoluble in the reaction medium but soluble in more polar solvents such as dimethylsulfoxide (DMSO). It was found by solution-state NMR that the desilylation reaction does not proceed once the intermediate products precipitate. Therefore, they have to be isolated, dissolved in DMSO, and treated with TBAF for a second time to ensure complete removal of the TDMS protecting groups. A determination of

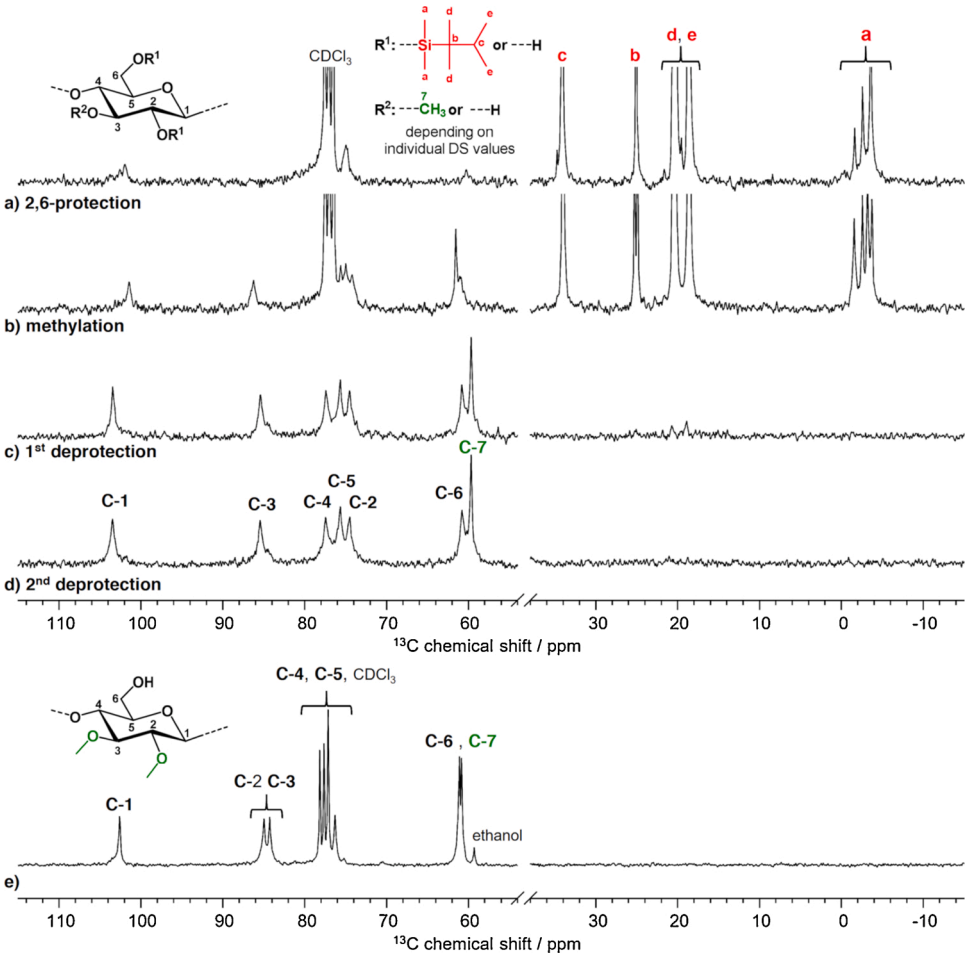

Fig. 2. (a) - (d) ^{13}C NMR spectra of the reaction products obtained in the different steps of the regioselective synthesis of 3-*O*-methylcellulose, recorded in solution in chloroform-d_1 (2,6-protection and methylation) or DMSO-d_6 with LiCl (1st and 2nd deprotection). **(e)** ^{13}C NMR spectra of 2,3-*O*-dimethylcellulose, recorded in solution in a mixture of methanol-d_1 and chloroform-d_1.

DS_{Me} from solution-state ^{1}H NMR spectra of cellulose ethers is usually not possible because the peaks related to the unmodified hydroxyl groups overlap with the peaks related to the cellulose repeating unit. Thus, a small portion of each product was peracetylated. This approach enabled direct determination of the DS_{Me} by solution-state ^{1}H NMR spectroscopy (Tezuka, Imai, Oshima, & Chiba, 1990).

3.2. NMR spectroscopic characterization of regioselective methylcelluloses in solution

All compounds synthesized were initially characterized using solution-state NMR. In this context it should be noted that the methylcellulose model compounds showed poor solubility in water and dipolar aprotic solvents, which is an indication for a very uniform molecular structure that induces strong intermolecular interactions of the polymers chain. DMSO-d_6 with LiCl was employed as solvent for 3-*O*-methylcellulose and a 4:1 mixture of methanol-d_4 and chloroform-d_1 was used to dissolve 2,3-*O*-dimethylcellulose. As shown in Fig. 2a, the ^{13}C NMR spectrum of TDMS cellulose showed the typical peaks of the cellulose backbone between 60 and 110 ppm, as well as characteristic peaks in the range of 35 to 20 ppm and at about -2 ppm that were assigned to the carbon atoms of the TDMS group according to literature (Heinze, Wang, Koschella, Sullo, & Foster, 2012; Ziegler, Bien, & Jurisch, 1998). In the spectrum of the mixed alky silyl cellulose ether (Fig. 2b), two new peaks are present. The one at about 59.7 ppm can be assigned to the carbon atom of the newly introduced methyl group (Koschella, Fenn, & Heinze, 2006) and the second peak at about 85 ppm was attributed by means of two-dimensional HSQC NMR to a cellulose carbon atom in position 3 bearing a methyl ether group. The intensity of the peaks related to the TDMS moiety decreased significantly after the first deprotection step but residues of the protecting group could still be detected and their complete removal was achieved after the second deprotection step.

The ^{13}C NMR spectrum of the 3-*O*-methylcellulose with a DS_{Me} of 0.99 showed seven individual peaks that were assigned to the six carbon atoms within the cellulose repeating unit and to the one carbon atom of the methyl group (Fig. 2d). This is a strong indication of the desired uniform molecular structure of a regioselectively substituted cellulose derivative. For the 2,3-*O*-dimethylcellulose (DS = 2.03), a similar ^{13}C NMR spectrum was recorded (see Fig. 2e). However, two peaks instead of one were observed in the range of about 87 ppm, which corresponded to the methylated C-2 and C-3 position. The peracetylated methylcelluloses were also analyzed by solution state NMR spectroscopy (see **Fig. S1**). It has been reported that the chemical shift of the peaks related to the carbonyl carbon atom of the acetyl group is sensitive to the location of the ester moiety within the repeating unit (Buchanan, Edgar, Hyatt, & Wilson, 1991). The spectrum of the peracetylated 3-*O*-dimethylcellulose sample featured only one peak in the carbonyl region located at 170.5 ppm, which is characteristic for an acetyl group in position 6. Two peaks in the carbonyl region could be identified in the spectrum of the peracetylated 3-*O*-methylcellulose sample at 170.5 ppm (acetyl group in position 6) and 169.5 ppm (acetyl group in position 2). This indirectly confirms the methylation of cellulose at the positions C-3 as well as C-2 and C-3 in the respective methylcellulose model compounds-.

3.3. NMR spectroscopic characterization of regioselective methylcelluloses in the solid-state with DNP CP-INADEQUATE

To further characterize the materials and develop a method for solid-state characterization, which can be used to analyze industrial cellulose ethers with unknown distribution patterns, the characterization of the reference samples in the solid-state with DNP enhanced solid-state NMR spectroscopy was studied. In 2009, Karrasch et al. studied uniform samples of 2-*O*-, 3-*O*-, and 6-*O*-methylcellulose obtained by cationic ring opening polymerization with solid-state NMR (Karrasch et al., 2009). The authors showed that the methyl ^{13}C signal can be efficiently selected through a rotor-synchronized dipolar dephasing experiment. They found for the three samples, that the CH_3 signal overlaps with the C-6 signal (see Fig. 2 for the atom labelling) with chemical shifts ranging from 59.8 ppm (6-*O*-methylcellulose) to 62.3 ppm (2-*O*-methylcellulose), and 62.4 ppm (3-*O*-methylcellulose). The resolution of the ^{13}C solid-state NMR spectrum of cellulose is usually not sufficient to capture such small chemical shift differences, and the authors attempted to use the ^{13}C T_1 relaxation rate of the substitution site to identify the latter. However, as we will show below, this relaxation rate approach may not be reliable. Here, an alternative method to identity the substitution pattern based on DNP NMR is proposed.

Although the chemical shift of the methyl function is not a discriminator for the substitution site (Karrasch et al., 2009), one can notice from the solution-state NMR spectroscopy of methylcellulose above that the chemical shifts of the carbon atoms within the cellulose repeating unit itself are affected by the substitution. Thus, full assignment of the chemical shifts of the ^{13}C signals in the solid-state should be sufficient to identify the substitution site. A simple and attractive approach to complete assignment of the carbon atoms in the cellulose repeating unit was introduced on ^{13}C enriched cellulose using ^{13}C-^{13}C CP-refocused-INADEQUATE experiments by Lesage et al.(Lesage, Bardet, & Emsley, 1999). This approach has been used subsequently (Kono, Erata, & Takai, 2003) but it suffers from low sensitivity and typically requires days long acquisition times. To address this it was shown that DNP can be adapted to NMR of powdered solids (Rossini et al., 2012) and De Paëpe and co-workers showed that DNP can be efficiently used on microcrystalline cellulose, with the report of ^{13}C-^{13}C DQ/SQ spectra recorded with the POST-C7 sequence in 20 min (Takahashi et al., 2012).

In DNP MAS, the sample is typically impregnated with a solution containing a polarizing agent, such as the bis-nitroxide AMUPOL used in this work (Sauvee et al., 2013), frozen at a temperature around 100 K, and then spun at the magic-angle under μwaves irradiation to induce DNP hyperpolarization (Rossini et al., 2013). The reference 3-*O*-methylcellulose sample was thus impregnated with a 10 mM AMUPOL solution in D_2O:H_2O $9{:}1_{v/v}$. As previously observed elsewhere (Kumar et al., 2020; Viger-Gravel et al., 2019), no cryoprotectant was used in the sample formulation, as the cellulose ether particles directly play this role. Fig. 3**a** (black) reports the ^{1}H-^{13}C DNP CPMAS NMR spectrum of the impregnated 3-*O*-methylcellulose. A ^{1}H DNP enhancement of 16 was measured on the cellulose sample through CP, which is consistent with the fact that the sample has a high concentration of methyl moieties, acting as polarization sinks (Zagdoun et al., 2013). Between 0 ppm and 40 ppm, low intensity signals are detected and have been presumed to be impurities left from the synthesis (the full spectrum is shown in **Fig S3**).

Fig. 3**a** (red) shows the ^{1}H-^{13}C DNP CPMAS NMR spectrum with the dipolar dephasing technique proposed in ref(Karrasch et al., 2009). In essence, this filter allows to extract the CH_3 signals of the methylcellulose ether. It consists of performing a ^{13}C spin echo over a few milliseconds following the CP transfer, without ^{1}H-^{13}C heteronuclear decoupling. Because the T_2' of CH and CH_2 are significantly more reduced by the absence of decoupling than the T_2' of CH_3, the latter is the only one to survive the filter (Karrasch et al., 2009; Opella & Frey, 1979; Wu, Burns, & Zilm, 1994). Here it allows to efficiently select the CH_3 signal, which overlaps with C-6. Although it does not allow to identify the substitution site, the experiment clearly corroborates that the sample is a methylcellulose ether.

The DNP enhancement was high enough to achieve good sensitivity and thus enable the recording of ^{13}C-^{13}C through bond (J coupling) correlation at natural abundance using the CP-refocused-INADEQUATE experiment (Lesage et al., 1999; Rossini et al., 2012). As depicted in Fig. 3b, this experiment allows straightforward assignment of the different carbons of the cellulose repeating unit of 3-*O*-methylcellulose. The resulting ^{13}C chemical shifts are provided in Table 1.

Comparing with the ^{13}C assignment of native cellulose, one first observes there is no co-existence of amorphous and crystalline regions in the sample. The signal assignments match with the assignments

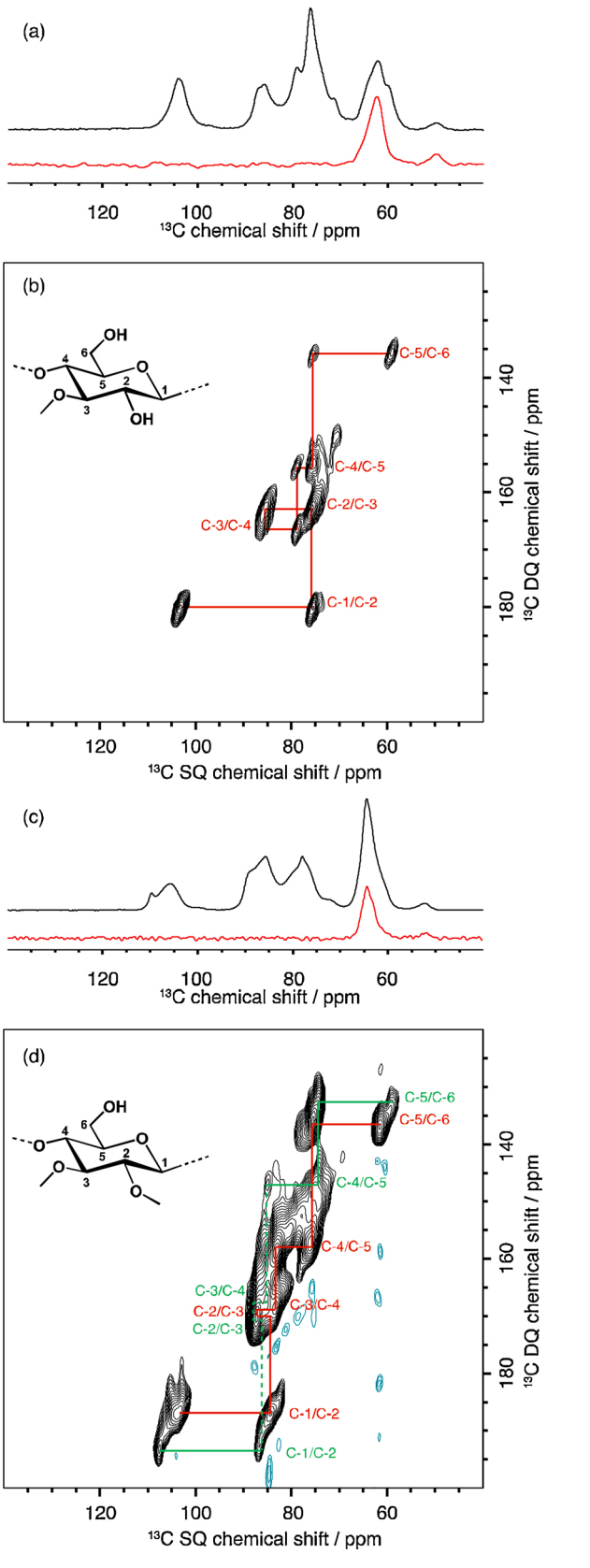

(caption on next column)

Fig. 3. **(a)** ^{1}H-^{13}C DNP CPMAS NMR spectrum (black) and ^{1}H-^{13}C DNP CPMAS NMR spectrum with CH_3 selection (red), and **(b)** ^{13}C-^{13}C DNP CP-refocused-INADEQUATE NMR spectrum of 3-*O*-methylcellulose impregnated with 10 mM AMUPOL in D_2O:H_2O 9:1$_{v/v}$, at 10 kHz MAS and at ca. 100 K. The red path indicates the correlations assigning the ^{13}C NMR spectrum. **(c)** ^{1}H-^{13}C DNP CPMAS NMR spectrum (black) and ^{1}H-^{13}C DNP CPMAS NMR spectrum with CH_3 selection (red), and **(d)** ^{13}C-^{13}C DNP CP-refocused-INADEQUATE NMR spectrum of 2,3-*O*-dimethylcellulose impregnated with 10 mM AMUPOL in D_2O/H_2O, at 10 kHz MAS and at ca. 100 K. The red and green paths indicate the correlations to assign the ^{13}C spectrum. The red path is assigned to an amorphous phase of 2,3-*O*-dimethylcellulose, whereas the green is proposed to belong to a crystalline phase. The dashed green line denotes a possible uncertainty in the path.

obtained with liquid state NMR and previous reports in the literature (Kono, Anai, Hashimoto, & Shimizu, 2015). In particular, the C-3 signal is shifted to significantly higher chemical shift compared to native cellulose, giving a clear indication of the substitution site. More generally, full spectral assignments of cellulose ethers seem to be a reliable approach to assess the methylation site of the cellulose, as they provide sufficient resolution to assign signals on the amorphous polymer.

Finally, we note that the origin of the signal at 50 ppm is still unclear, and we are not able to provide an assignment. However, using conventional Solid-State NMR methods of the non-impregnated samples, we have discarded the possibility of a side reaction due to the presence of the DNP polarizing agent (see **Fig. S2**). We have observed similar signals on different samples from different origins (not shown), suggesting that it is not an impurity from the synthesis.

To benchmark the reliability of the identification of the methylation site through the measurement of ^{13}C chemical shifts with ^{13}C-^{13}C DNP enhanced CP-refocused-INADEQUATE, we also analyzed the 2,3-*O*-dimethylcellulose model compound with the same approach. Fig. 3**c** reports the ^{1}H-^{13}C DNP CPMAS NMR spectrum of the 2,3-*O*-dimethylcellulose (black) impregnated with 10 mM AMUPOL in D_2O:H_2O 9:1$_{v/v}$ and the ^{1}H-^{13}C DNP CPMAS NMR with CH_3 selection (red). Although the CH_3 selection shows the presence of the methoxy groups in the samples, their chemical shifts in a 1D experiment are too close to allow individual identification of the methylation sites. Fig. 3**d** reports the ^{13}C-^{13}C DNP enhanced CP-refocused-INADEQUATE of the 2,3-*O*-dimethylcellulose. Two separate pathways of correlation have been assigned and are reported on Fig. 3**d** (in green and red). Similarly, to microcrystalline cellulose, we assign these two systems to the co-existence of a crystalline (green) and an amorphous (red) phase of 2,3-*O*-dimethylcellulose. The aspect of the C-1 signal (narrow peak at 107.5 ppm and broader peak at 103.5 ppm) is typical of the presence of both crystalline and amorphous cellulose (Atalla & Vanderhart, 1984; Foston, 2014; Wickholm, Hult, Larsson, Iversen, & Lennholm, 2001). The ^{13}C chemical shifts of the two spin systems are reported in Table 1. Note the uncertainty of the assignments of crystalline-C-3 and crystalline-C-4 is indicated using dashed green lines in Fig. 3**d** and italics in Table 1. Compared to microcrystalline cellulose, we can see that both C-2 and C-3 are shifted to higher chemical shifts, regardless of if they are in the amorphous or crystalline phase. This clearly identifies the methylation sites as C-2 and C-3. The fact that they both shifted is also a clear indication that we are indeed looking at two phases of 2, 3-*O*-dimethylcellulose, and not 2,3-*O*-dimethylcellulose with an unreacted cellulose impurity. Thus, this example illustrates nicely how the sensitivity provided by DNP enables chemical shift assignments *via* the ^{13}C-^{13}C CP-refocused-INADEQUATE experiment at natural abundance, and in consequence how the substitution sites can be simply identified based on the difference of the ^{13}C chemical shifts with respect to native cellulose.

Table 1
^{13}C chemical shifts of the cellulose ethers 3-*O*-methylcellulose **(3-*O*-MeC)**, and 2,3-*O*-dimethylcellulose **(2,3-*O*-diMeC)** determined from the ^{13}C-^{13}C DNP CP-refocused INADEQUATE NMR spectra and ^{1}H-^{13}C DNP CPMAS NMR spectrum with CH_3 selection. The ^{13}C chemical shifts of microcrystalline cellulose **(MCC)** are taken from the literature(Lesage et al., 1999). Chemical shifts for the crystalline **(c)** and amorphous phase **(a)** of **2,3-*O*-diMeC** are given. For **MCC**, the amorphous/surface phase C-4 signal has been reported with lower chemical shift, thus **(c)/(a)** chemical shifts are reproduced here. ^{13}C chemical shifts are provided using the tetramethylsilane reference scale.

Sample		Chemical shift, ppm						
		C-1	C-2	C-3	C-4	C-5	C-6	CH_3
3-*O*-MeC		103.1	75.4	85.8	78.7	75.4	59.1	63.1
2,3-*O*-diMeC	**c**	107.5	86.6	*87.5*	*85.4*	74.6	59.2	62.2
	a	103.5	84.4	87.3	83.2	75.5	61.6	
MCC	**c**	105	73	74.5	87	74.5	62	–
	a				≈ 82			

3.4. NMR spectroscopic characterization of 3-O-methylcellulose in the solid-state with DNP hNOE

While spectral assignments via DNP CP-INADEQUATE revealed the substitution site of the cellulose ethers, we also explored the possibility to directly correlate the methyl group with the nearby substitution site on the cellulose backbone. In particular, CH_3 groups are peculiar in the DNP MAS context. Because of the fast rotation of the CH_3 group, even at 100 K, the latter is known to *(i)* act as a relaxation sink which depreciates the DNP enhancements, explaining why materials that contain CH_3 usually exhibit low DNP performance (Zagdoun et al., 2013), *(ii)* ^{1}H-^{13}C CP conditions of CH_3 are very sensitive to the temperature in the 100 K range, this has been reported in polymers where the temperature difference induced by the μwaves absorption can induce a bias in the enhancement measurement (Mollica et al., 2014), and *(iii)* induce spontaneous transfer from ^{1}H to ^{13}C through heteronuclear Nuclear Overhauser Effect (hNOE) (Aladin & Corzilius, 2019; Daube et al., 2016; Mao et al., 2019). In 2019, Corzilius and co-workers showed that uniformly ^{13}C-enriched amino acids can be hyperpolarized using hNOE together with spontaneous ^{13}C-^{13}C spin diffusion. In the context of characterization of methylcellulose, this is of particular interest, as hNOE can selectively and spontaneously hyperpolarize the grafted CH_3. The strategy we propose here relies on the extension of DNP hNOE to non-labelled cellulose ethers in order to localize the substitution site. As pictured in Fig. 4a, ^{1}H nuclei of the solvent are hyperpolarized directly by the AMUPOL polarizing agent. Then, as established previously (Pinon et al., 2017), the ^{1}H hyperpolarization diffuses through the sample via spontaneous ^{1}H-^{1}H spin diffusion and eventually reaches the ^{1}H of the cellulose including the CH_3 moiety. Because of the hNOE effect, the ^{1}H hyperpolarization of the CH_3 then spontaneously transfers to the ^{13}C of the CH_3. The ^{13}C hyperpolarization can then be further transmitted via ^{13}C-^{13}C spin diffusion. As we are working with ^{13}C at natural abundance, in principle ^{13}C spin diffusion will only transfer polarization to the closest carbons in space (including the substitution site) of the hyperpolarized CH_3. Using the model reported in the literature (Bjorgvinsdottir, Walder, Pinon, & Emsley, 2018), it was possible to estimate that the ^{13}C spin diffusion will only probe from 4 to 9 Å with a transfer delay of 1 to 5 s at 10 kHz MAS.

Fig. 4**b** shows the ^{13}C DNP direct excitation spectra recorded with and without μwaves on a sample of 3-*O*-methylcellulose impregnated with 10 mM AMUPOL at different recycle delays. Identical phase correction parameters were used to process all the spectra. Direct ^{13}C DNP will offer a positive DNP enhancement (Kaushik et al., 2016), whereas hNOE is expected to provide a ^{13}C negative DNP enhancement (Daube et al., 2016). Thus, hNOE is the main active DNP transfer here. Fig. 4**c** is the ^{1}H-^{13}C DNP CPMAS of the same sample at 5 kHz MAS, displayed for comparison with the direct ^{13}C spectra, one can observe the predominance of the CH_3 signals in 4b due to the direct hNOE DNP

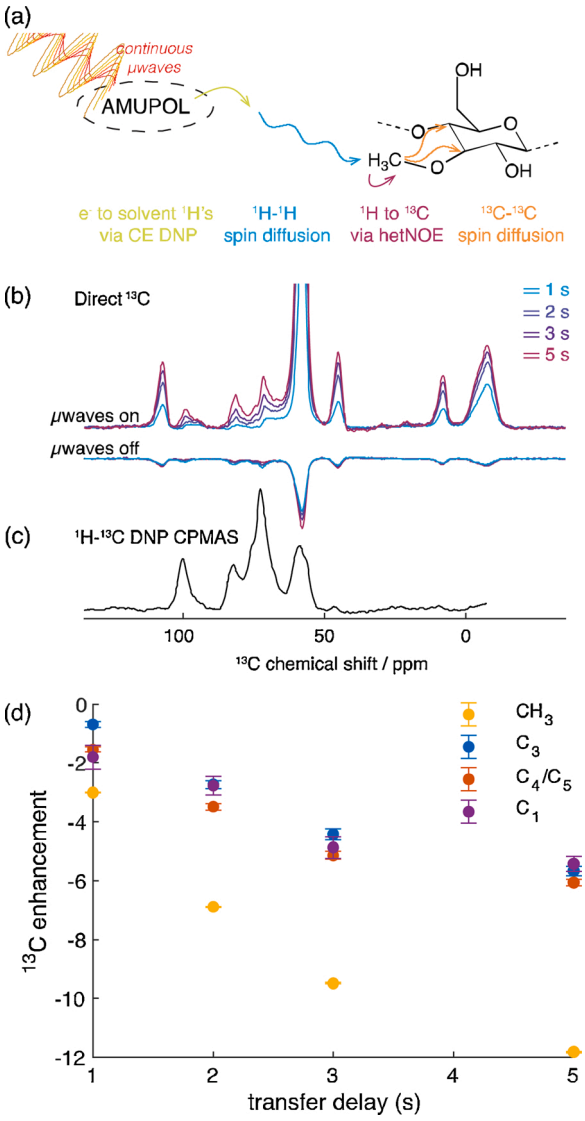

Fig. 4. (a) Principle of substitution site identification for the reference sample 3-*O*-methylcellulose by combining DNP MAS with hNOE and ^{13}C-^{13}C spin diffusion. (b) Direct ^{13}C NMR spectra with (plain line) and without (dashed line) μwave irradiation, and with recycle delays varying from 1 to 5 s and (c) ^{1}H-^{13}C DNP CPMAS of 3-*O*-methylcellulose impregnated with 10 mM AMUPOL in D_2O:H_2O 9:1$_{v/v}$ at 5 kHz MAS, at ca. 100 K. (d) ^{13}C enhancement (from direct ^{13}C NMR) as function of the recycle delay and for the different resolved and detectable signals.

enhancement route. As all signals are negative, and we can then expect the process described in Fig. 4**a** to be predominant, *i.e.,* ^{13}C gets hyperpolarized via ^{13}C-^{13}C spin diffusion from the CH_3 functionality. Fig. 4**d** reports the ^{13}C signal enhancements of the different detectable and resolved signals: CH_3, C-1, C-3, and C-4/C-5 as a function of the ^{13}C spin diffusion delay. Note particularly that C-2 and C-6 signals are not observable in the direct ^{13}C spectra. As only C-1, C-3, and C-4/C-5 are detectable, we can conclude that they are the closest carbons in space to CH_3. Among them, only C-3 can be etherified, and thus it implies that the substitution site is C-3. Although the signal assignments of the 3-*O*-methylcellulose from the ^{13}C-^{13}C INADEQUATE already gives a clear answer regarding the substitution site, the strategy based on hNOE also seems to identify the substitution site.

4. Conclusion

Using a multistep synthesis approach and protecting group strategies, two methylcellulose ethers with a well-defined molecular structure were prepared, one with a regioselective 3-*O*-substitution ($DS_{Me} = 0.99$) and one with regioselective 2,3-*O*-substitution ($DS_{Me} = 2.03$). These model compounds were used to introduce and benchmark two new solid-state NMR based approaches that allow to characterize the substitution pattern in cellulose ethers. The first method uses the ^{13}C chemical shift assignments of the cellulose ether via ^{13}C-^{13}C DNP enhanced refocused INADEQUATE. It gives a particularly clear identification of the substitution site on both 3-*O*-methylcellulose and 2,3-*O*-dimethylcellulose, and should be generalizable to any cellulose ether. The assignments are made possible in the solid-state because of the sensitivity enhancement due to the use of DNP MAS. The second method is based on selective hyperpolarization of CH_3 via hNOE and subsequent transfer via ^{13}C spin diffusion at natural abundance, which also allow to confirm the postulated regioselectivity within the model compounds.

Author contributions

This work was produced through contributions of all authors to the conception, implementation, analysis and writing of the paper.

Acknowledgment

This work was financially supported by the Swiss Innovation Agency Innosuisse (Grant: 30819.1 IP-ENG).

Appendix A. Supplementary data

Supplementary material related to this article can be found, in the online version, at doi:https://doi.org/10.1016/j.carbpol.2021.117944.

References

Aladin, V., & Corzilius, B. (2019). Methyl dynamics in amino acids modulate heteronuclear cross relaxation in the solid state under MAS DNP. *Solid State Nuclear Magnetic Resonance, 99*, 27–35.

Arca, H. C., Mosquera-Giraldo, L. I., Bi, V., Xu, D., Taylor, L. S., & Edgar, K. J. (2018). Pharmaceutical applications of cellulose ethers and cellulose ether esters. *Biomacromolecules, 19*(7), 2351–2376.

Atalla, R. H., & Vanderhart, D. L. (1984). Native cellulose: A composite of two distinct crystalline forms. *Science, 223*(4633), 283–285.

Berruyer, P., Emsley, L., & Lesage, A. (2018). DNP in materials science: Touching the surface. *Emagres, 7*(4), 93–104.

Bjorgvinsdottir, S., Walder, B. J., Pinon, A. C., & Emsley, L. (2018). Bulk nuclear hyperpolarization of inorganic solids by relay from the surface. *Journal of the American Chemical Society, 140*(25), 7946–7951.

Buchanan, C. M., Edgar, K. J., Hyatt, J. A., & Wilson, A. K. (1991). Preparation of cellulose [1-carbon-13]acetates and determination of monomer composition by NMR spectroscopy. *Macromolecules, 24*(11), 3050–3059.

Daube, D., Aladin, V., Heiliger, J., Wittmann, J. J., Barthelmes, D., Bengs, C., et al. (2016). Heteronuclear cross-relaxation under solid-state dynamic nuclear polarization. *Journal of the American Chemical Society, 138*(51), 16572–16575.

Elkins, M. R., Sergeyev, I. V., & Hong, M. (2018). Determining cholesterol binding to membrane proteins by cholesterol ^{13}C labeling in yeast and dynamic nuclear polarization NMR. *Journal of the American Chemical Society, 140*(45), 15437–15449.

Foston, M. (2014). Advances in solid-state NMR of cellulose. *Current Opinion in Biotechnology, 27*, 176–184.

Foston, M., Katahira, R., Gjersing, E., Davis, M. F., & Ragauskas, A. J. (2012). Solid-state selective (13)C excitation and spin diffusion NMR to resolve spatial dimensions in plant cell walls. *Journal of Agricultural and Food Chemistry, 60*(6), 1419–1427.

Fox, S. C., Li, B., Xu, D., & Edgar, K. J. (2011). Regioselective esterification and etherification of cellulose: A review. *Biomacromolecules, 12*(6), 1956–1972.

Groszewicz, P. B., Mendes, P., Kumari, B., Lins, J., Biesalski, M., Gutmann, T., et al. (2020). N-hydroxysuccinimide-activated esters as a functionalization agent for amino cellulose: Synthesis and solid-state NMR characterization. *Cellulose, 27*(3), 1239–1254.

Gupta, R., Zhang, H. L., Lu, M. M., Hou, G. J., Caporini, M., Rosay, M., et al. (2019). Dynamic nuclear polarization magic-angle spinning nuclear magnetic resonance combined with molecular dynamics simulations permits detection of order and disorder in viral assemblies. *The Journal of Physical Chemistry B, 123*(24), 5048–5058.

Heinze, T., Pfeifer, A., Sarbova, V., & Koschella, A. (2011). 3-*O*-propyl cellulose: Cellulose ether with exceptionally low flocculation temperature. *Polymer Bulletin, 66*(9), 1219–1229.

Heinze, T., Wang, Y., Koschella, A., Sullo, A., & Foster, T. J. (2012). Mixed 3-mono-*O*-alkyl cellulose: Synthesis, structure characterization and thermal properties. *Carbohydrate Polymers, 90*(1), 380–386.

Kang, X., Kirui, A., Widanage, M. C. D., Mentink-Vigier, F., Cosgrove, D. J., & Wang, T. (2019). Lignin-polysaccharide interactions in plant secondary cell walls revealed by solid-state NMR. *Nature Communications, 10*.

Karlson, L., Joabsson, F., & Thuresson, K. (2000). Phase behavior and rheology in water and in model paint formulations thickened with HM-EHEC: Influence of the chemical structure and the distribution of hydrophobic tails. *Carbohydrate Polymers, 41*(1), 25–35.

Karrasch, A., Jager, C., Karakawa, M., Nakatsubo, F., Potthast, A., & Rosenau, T. (2009). Solid-state NMR studies of methyl celluloses. Part 1: Regioselectively substituted celluloses as standards for establishing an NMR data basis. *Cellulose, 16*(1), 129–137.

Kaushik, M., Bahrenberg, T., Can, T. V., Caporini, M. A., Silvers, R., Heiliger, J., et al. (2016). Gd(III) and Mn(II) complexes for dynamic nuclear polarization: Small molecular chelate polarizing agents and applications with site-directed spin labeling of proteins. *Physical Chemistry Chemical Physics, 18*(39), 27205–27218.

Kern, H., Choi, S., Wenz, G., Heinrich, J., Ehrhardt, L., Mischnick, P., et al. (2000). Synthesis, control of substitution pattern and phase transitions of 2,3-di-*O*-methylcellulose. *Carbohydrate Research, 326*(1), 67–79.

Kondo, T., & Gray, D. G. (1991). The preparation of *O*-methyl- and *O*-ethyl-celluloses having controlled distribution of substituents. *Carbohydrate Research, 220*(0), 173–183.

Kono, H., Anai, H., Hashimoto, H., & Shimizu, Y. (2015). ^{13}C-detection two-dimensional NMR approaches for cellulose derivatives. *Cellulose, 22*(5), 2927–2942.

Kono, H., Erata, T., & Takai, M. (2002). CP/MAS ^{13}C NMR study of cellulose and cellulose derivatives. 2. Complete assignment of the ^{13}C resonance for the ring carbons of cellulose triacetate polymorphs. *Journal of the American Chemical Society, 124*(25), 7512–7518.

Kono, H., Erata, T., & Takai, M. (2003). Determination of the through-bond carbon-carbon and carbon-proton connectivities of the native celluloses in the solid state. *Macromolecules, 36*(14), 5131–5138.

Kono, H., Numata, Y., Erata, T., & Takai, M. (2004). ^{13}C and ^{1}H resonance assignment of mercerized cellulose II by two-dimensional MAS NMR spectroscopies. *Macromolecules, 37*(14), 5310–5316.

Koschella, A., & Klemm, D. (1997). Silylation of cellulose regiocontrolled by bulky reagents and dispersity in the reaction media. *Macromolecular Symposia, 120*(1), 115–125.

Koschella, A., Heinze, T., & Klemm, D. (2001). First synthesis of 3-*O*-functionalized cellulose ethers via 2,6-di-*O*-protected silyl cellulose. *Macromolecular Bioscience, 1*(1), 49–54.

Koschella, A., Fenn, D., & Heinze, T. (2006). Water soluble 3-mono-*O*-ethyl cellulose: Synthesis and characterization. *Polymer Bulletin, 57*(1), 33–41.

Koschella, A., Fenn, D., Illy, N., & Heinze, T. (2006). Regioselectively functionalized cellulose derivatives: A mini review. *Macromolecular Symposia, 244*(1), 59–73.

Kumar, A., Durand, H., Zeno, E., Balsollier, C., Watbled, B., Sillard, C., et al. (2020). The surface chemistry of a nanocellulose drug carrier unravelled by MAS-DNP. *Chemical Science, 11*(15), 3868–3877.

Lesage, A., Bardet, M., & Emsley, L. (1999). Through-bond carbon-carbon connectivities in disordered solids by NMR. *Journal of the American Chemical Society, 121*(47), 10987–10993.

Li, C. L., Martini, L. G., Ford, J. L., & Roberts, M. (2005). The use of hypromellose in oral drug delivery. *The Journal of Pharmacy and Pharmacology, 57*(5), 533–546.

Mao, J. F., Aladin, V., Jin, X. S., Leeder, A. J., Brown, L. J., Brown, R. C. D., et al. (2019). Exploring protein structures by dnp-enhanced methyl solid-state NMR spectroscopy. *Journal of the American Chemical Society, 141*(50), 19888–19901.

Mischnick, P. (2018). *Analysis of the substituent distribution in cellulose ethers - recent contributions: Chemistry, analysis, and applications* (pp. 143–173).

Mollica, G., Le, D., Ziarelli, F., Casano, G., Ouari, O., Phan, T. N. T., et al. (2014). Observing apparent nonuniform sensitivity enhancements in dynamic nuclear polarization solid-state NMR spectra of polymers. *ACS Macro Letters, 3*(9), 922–925.

Opella, S. J., & Frey, M. H. (1979). Selection of non-protonated carbon resonances in solid-state nuclear magnetic-resonance. *Journal of the American Chemical Society, 101*(19), 5854–5856.

Patural, L., Marchal, P., Govin, A., Grosseau, P., Ruot, B., & Devès, O. (2011). Cellulose ethers influence on water retention and consistency in cement-based mortars. *Cement and Concrete Research, 41*(1), 46–55.

Perras, F. A., Luo, H., Zhang, X. M., Mosier, N. S., Pruski, M., & Abu-Omar, M. M. (2017). Atomic-level structure characterization of biomass pre- and post-lignin treatment by dynamic nuclear polarization-enhanced solid-state NMR. *The Journal of Physical Chemistry A, 121*(3), 623–630.

Pinon, A. C., Schlagnitweit, J., Berruyer, P., Rossini, A. J., Lelli, M., Socie, E., et al. (2017). Measuring nano- to microstructures from relayed dynamic nuclear polarization NMR. *The Journal of Physical Chemistry C, 121*(29), 15993–16005.

Reif, B., Ashbrook, S. E., Emsley, L., & Hong, M. (2021). Solid-state NMR spectroscopy. *Nature Reviews Methods Primers, 1*(1), 2.

Rossini, A. J., Zagdoun, A., Hegner, F., Schwarzwalder, M., Gajan, D., Coperet, C., et al. (2012). Dynamic nuclear polarization NMR spectroscopy of microcrystalline solids. *Journal of the American Chemical Society, 134*(40), 16899–16908.

Rossini, A. J., Zagdoun, A., Lelli, M., Lesage, A., Coperet, C., & Emsley, L. (2013). Dynamic nuclear polarization surface enhanced NMR spectroscopy. *Accounts of Chemical Research, 46*(9), 1942–1951.

Sauvee, C., Rosay, M., Casano, G., Aussenac, F., Weber, R. T., Ouari, O., et al. (2013). Highly efficient, water-soluble polarizing agents for dynamic nuclear polarization at high frequency. *Angewandte Chemie-International Edition, 52*(41), 10858–10861.

Schmidt-Rohr, K., & Spiess, H. W. (1999). *Multidimensional solid-state NMR and polymers* (third printing ed.). London etc: Academic Press.

Sparrman, T., Svenningsson, L., Sahlin-Sjovold, K., Nordstierna, L., Westman, G., & Bernin, D. (2019). A revised solid-state NMR method to assess the crystallinity of cellulose. *Cellulose, 26*(17), 8993–9003.

Sun, S. M., Foster, T. J., MacNaughtan, W., Mitchell, J. R., Fenn, D., Koschella, A., et al. (2009). Self-association of cellulose ethers with random and regioselective distribution of substitution. *Journal of Polymer Science Part B-Polymer Physics, 47*(18), 1743–1752.

Takahashi, H., Lee, D., Dubois, L., Bardet, M., Hediger, S., & De Paepe, G. (2012). Rapid natural-abundance 2D ^{13}C-^{13}C correlation spectroscopy using dynamic nuclear polarization enhanced solid-state NMR and matrix-free sample preparation. *Angewandte Chemie-International Edition, 51*(47), 11766–11769.

Tezuka, Y., Imai, K., Oshima, M., & Chiba, T. (1990). Determination of substituent distribution in cellulose ethers by ^{13}C- and ^{1}H-NMR. Studies of their acetylated derivatives: O-(2-hydroxypropyl)cellulose. *Carbohydrate Research, 196*, 1–10.

Viger-Gravel, J., Lan, W., Pinon, A. C., Berruyer, P., Emsley, L., Bardet, M., et al. (2019). Topology of pretreated wood fibers using dynamic nuclear polarization. *The Journal of Physical Chemistry C, 123*(50), 30407–30415.

Wang, T., Park, Y. B., Caporini, M. A., Rosay, M., Zhong, L. H., Cosgrove, D. J., et al. (2013). Sensitivity-enhanced solid-state NMR detection of expansin's target in plant cell walls. *Proceedings of the National Academy of Sciences of the United States of America, 110*(41), 16444–16449.

Wang, T., Yang, H., Kubicki, J. D., & Hong, M. (2016). Cellulose structural polymorphism in plant primary cell walls investigated by high-field 2D solid-state NMR spectroscopy and density functional theory calculations. *Biomacromolecules, 17*(6), 2210–2222.

Wever, D. A. Z., Picchioni, F., & Broekhuis, A. A. (2011). Polymers for enhanced oil recovery: A paradigm for structure–Property relationship in aqueous solution. *Progress in Polymer Science, 36*(11), 1558–1628.

Wickholm, K., Hult, E. L., Larsson, P. T., Iversen, T., & Lennholm, H. (2001). Quantification of cellulose forms in complex cellulose materials: A chemometric model. *Cellulose, 8*(2), 139–148.

Wu, X. L., Burns, S. T., & Zilm, K. W. (1994). Spectral editing in CPMAS NMR - generating subspectra based on proton multiplicities. *Journal of Magnetic Resonance Series A, 111*(1), 29–36.

Young, N. W. G. (2014). Emulsifiers and stabilisers. In K. K. Rajah (Ed.), *Fats in food technology 2e* (pp. 253–287). John Wiley & Sons, Ltd.

Zagdoun, A., Rossini, A. J., Conley, M. P., Gruning, W. R., Schwarzwalder, M., Lelli, M., et al. (2013). Improved dynamic nuclear polarization surface-enhanced NMR spectroscopy through controlled incorporation of deuterated functional groups. *Angewandte Chemie-International Edition, 52*(4), 1222–1225.

Zhao, W. C., Kirui, A., Deligey, F., Mentink-Vigier, F., Zhou, Y. H., Zhang, B. C., et al. (2021). Solid-state nmr of unlabeled plant cell walls: High-resolution structural analysis without isotopic enrichment. *Biotechnology for Biofuels, 14*(1).

Ziegler, T., Bien, F., & Jurisch, C. (1998). Chemoenzymatic synthesis of enantiomerically pure alkene 1,2-diols and glycosides thereof. *Tetrahedron: Asymmetry, 9*(5), 765–780.